eLIFE elifesciences.org

RESEARCH ARTICLE

Figures and figure supplements

Neurogliaform cortical interneurons derive from cells in the preoptic area

Mathieu Niquille *et al*

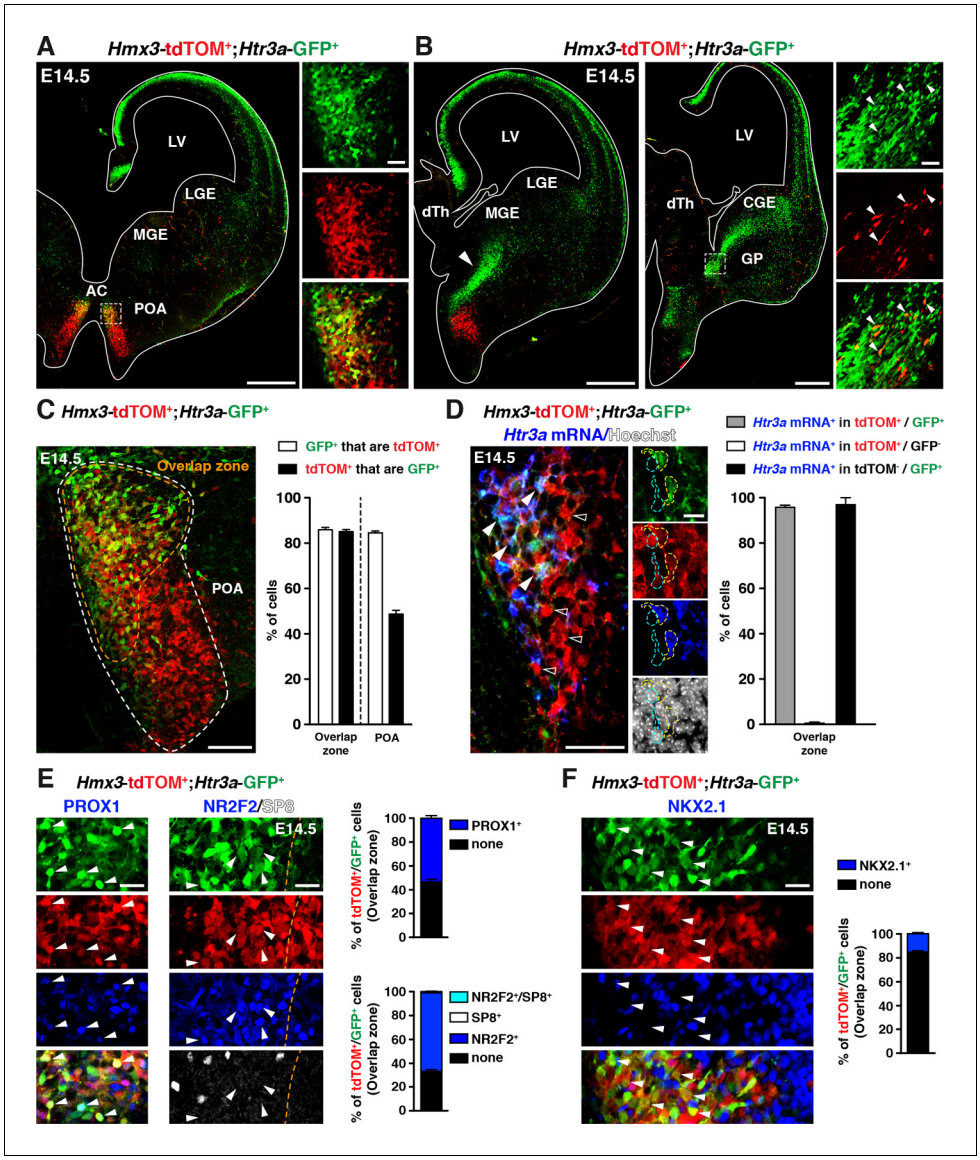

Figure 1. A fraction of 5-HT$_{3A}$R-expressing interneurons (INs) originates from *Hmx3*-derived cells in the preoptic area (POA) and expresses transcription factors related to the caudal ganglionic eminence (CGE). (**A**) At E14.5, tdTOM specifically labels cells expressing *Hmx3* (*Hmx3*; tdTOM+). *Htr3a*-GFP+ INs co-label with tdTOM in a rostral region of the POA (dashed lines; high magnified images) located ventrally to the anterior commissure (AC). (**B**) At more caudal levels, *Hmx3*; tdTOM+/*Htr3a*-GFP+ embryonic cells appear to further migrate caudally (arrowhead) towards the CGE. High magnified images show *Hmx3*; tdTOM+/*Htr3a*-GFP+ cells entering the ventral CGE (dashed lines). (**C**) More than 80% of *Hmx3*; tdTOM+ cells co-label with *Htr3a*-GFP (and conversely) in the overlap zone (orange dashed line) of the POA domain defined by *Hmx3*; tdTOM recombination (white dashed line). (**D**) *In situ* hybridization showing that almost all *Hmx3*; tdTOM+/*Htr3a*-GFP+ INs in the POA express the *Htr3a* mRNA (arrowheads; yellow outline), whereas *Hmx3*; tdTOM+ cells do not (empty arrowheads; cyan outline). (**E**) In the overlap zone of the POA, IHC reveals that *Hmx3*; tdTOM+/*Htr3a*-GFP+ embryonic cells express (arrowheads) the CGE-enriched transcription factors PROX1 (left) and NR2F2 but not SP8 (right). (**F**) By contrast, the vast majority of *Hmx3*; tdTOM+/*Htr3a*-GFP+ INs do not express NKX2.1 (arrowheads). dTh: dorsal thalamus, GP: globus pallidus, LGE: lateral ganglionic eminence, LV: lateral ventricle, MGE: medial ganglionic eminence. Scale bars: 300 µm in A, B: low magnified images; 100 µm in C, D: low magnified images; 50 µm in A, B: high magnified images; 25 µm in E, F; 10 µm in D: high magnified images.

DOI: https://doi.org/10.7554/eLife.32017.003

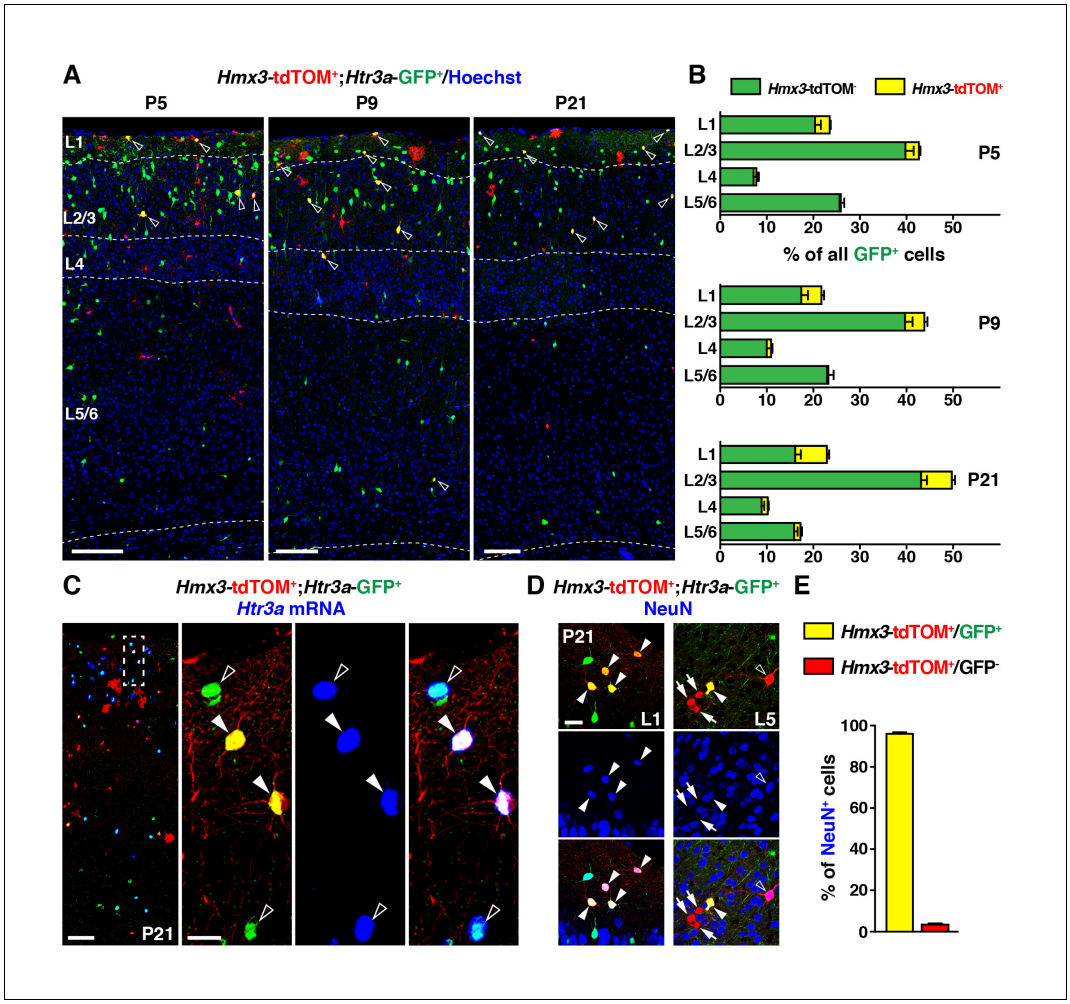

Figure 2. During the postnatal period, *Hmx3*-derived cells from the preoptic area (***Gelman et al., 2009***) constitute a small but persistent fraction of 5-HT_{3A}R-expressing interneurons (INs) (***Lee et al., 2010***) in superficial cortical layers. (**A–B**) *Hmx3*; tdTOM+/*Htr3a*-GFP+ cells represent a fraction of *Htr3a*-GFP+ INs that increases along postnatal ages P5 (left), P9 (middle) and P21 (right). Note that double-labeled cells (open arrowheads) are mainly located in superficial cortical layers. (**C**) *In situ* hybridization showing that, at P21, *Htr3a* mRNA is found in cortical *Hmx3*; tdTOM+/*Htr3a*-GFP+ INs (arrowheads) as in *Htr3a*-GFP+ INs (open arrowheads). (**D–E**) *Hmx3*; tdTOM+/*Htr3a*-GFP+ cells largely express the neuronal marker NeuN (arrowheads) whereas those negative for *Htr3a*-GFP only rarely do (arrows, open arrowhead). Scale bars: 100 μm in A, C: low magnified images; 25 μm in C: high magnified images, D.

DOI: https://doi.org/10.7554/eLife.32017.005

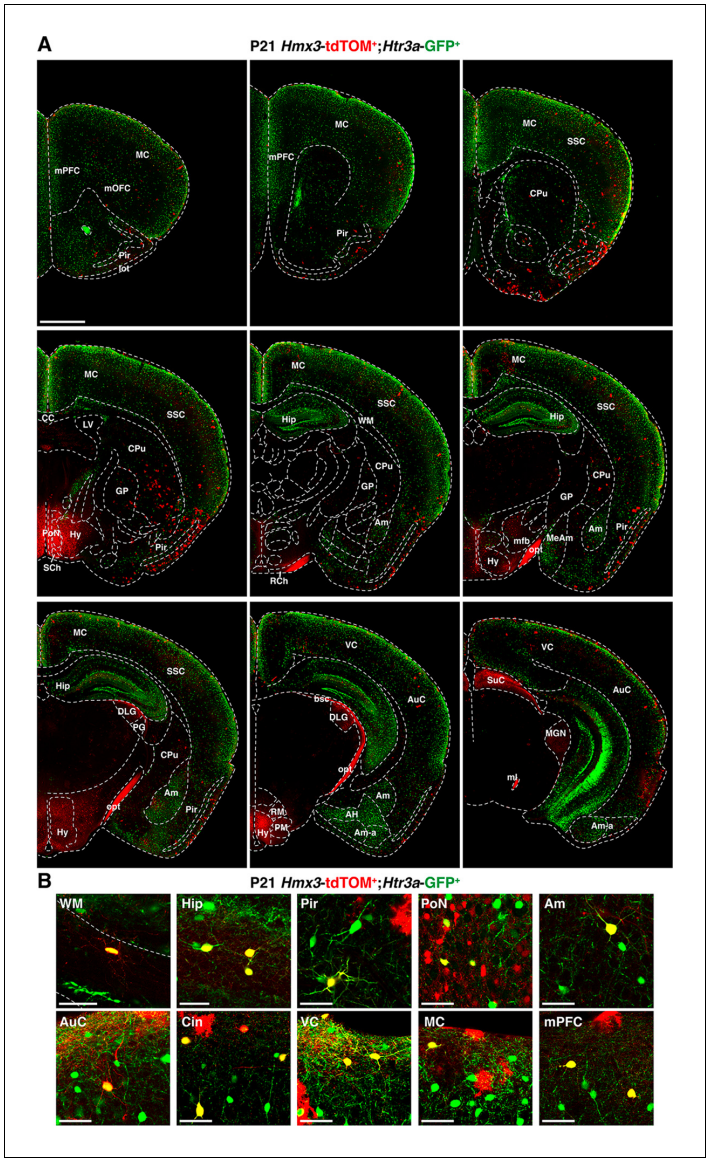

Figure 2—figure supplement 1. Rostro-caudal distribution of *Hmx3*; tdTOM+/*Htr3a*-GFP+ cells at P21. (**A**) *Hmx3*; tdTOM+/*Htr3a*-GFP+ cells are observed in a variety of cortical areas as well as other brain regions including the hippocampus (Hip) and the amygdala (Am) (**B**) High magnified images showing *Hmx3*; tdTOM+/*Htr3a*-GFP+ cells in various brain regions. AH: amygdalo-hippocampal area, Am-a: amygdaloid areas, AuC: auditory cortex, bsc: brachius of the superior colliculus, CC: corpus callosum, CPu: caudate putamen (striatum), DLG: dorso-lateral geniculate nucleus, GP: globus pallidus, Hy: hypothalamus, lot: lateral olfactory tract, LV: lateral ventricle, MC: motor cortex, MeAm: medial amygdala, mfb: medial forebrain boundle, ml: medial lemniscus, MGN: medial geniculate nucleus, mOFC: medial orbitofrontal cortex, mPFC: medial prefrontal cortex, opt: optic tract, PG: progeniculate nucleus, Pir: piriform cortex, PM: pre-mamillary nuclei, PoN: preoptic nucleus, RCh: retrochiasmatic area, RM: retro-mamillary nuclei, SCh: suprachiasmatic nucleus, SSC: somatosensory cortex, SuC: superior colliculus (optic nerve layer and superficial grey layer), VC: visual cortex, WM: white matter. Scale bars: 5 mm in A; 50 µm in B.

DOI: https://doi.org/10.7554/eLife.32017.006

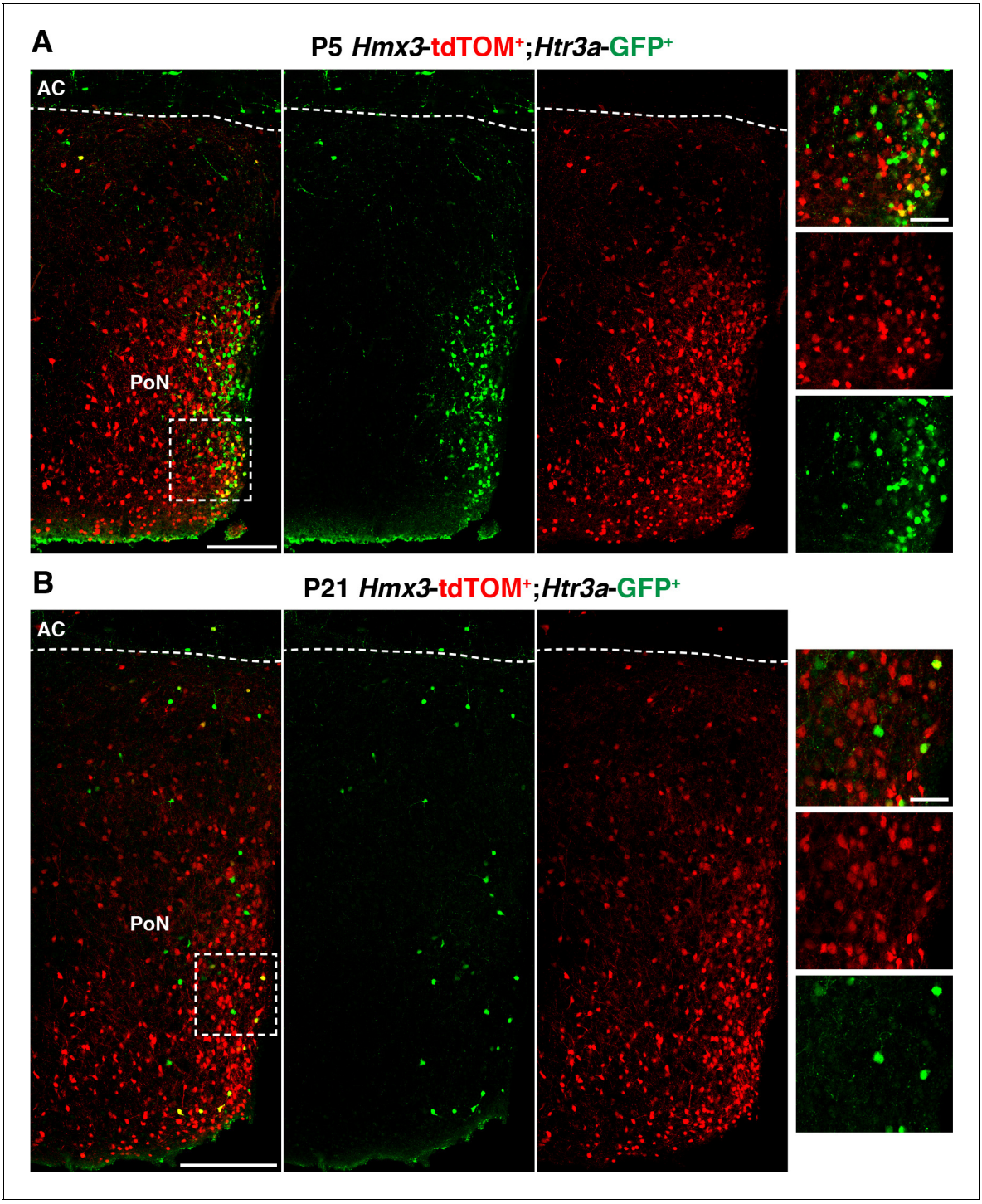

Figure 2—figure supplement 2. At postnatal ages, *Hmx3*; tdTOM+/*Htr3a*-GFP+ cells are rarely observed in the preoptic nuclei (PoN), the subpallial brain region corresponding to the embryonic preoptic area. (**A–B**) *Hmx3*; tdTOM+ cells negative for *Htr3a*-GFP are present in PoN at P5 (**A**), and P21 (**B**) where rare *Hmx3*; tdTOM+/*Htr3a*-GFP+ were found (high magnified images). AC: anterior commissure. Scale bars: 300 μm in A, B: low magnified images; 50 μm in A, B: high magnified images.

DOI: https://doi.org/10.7554/eLife.32017.007

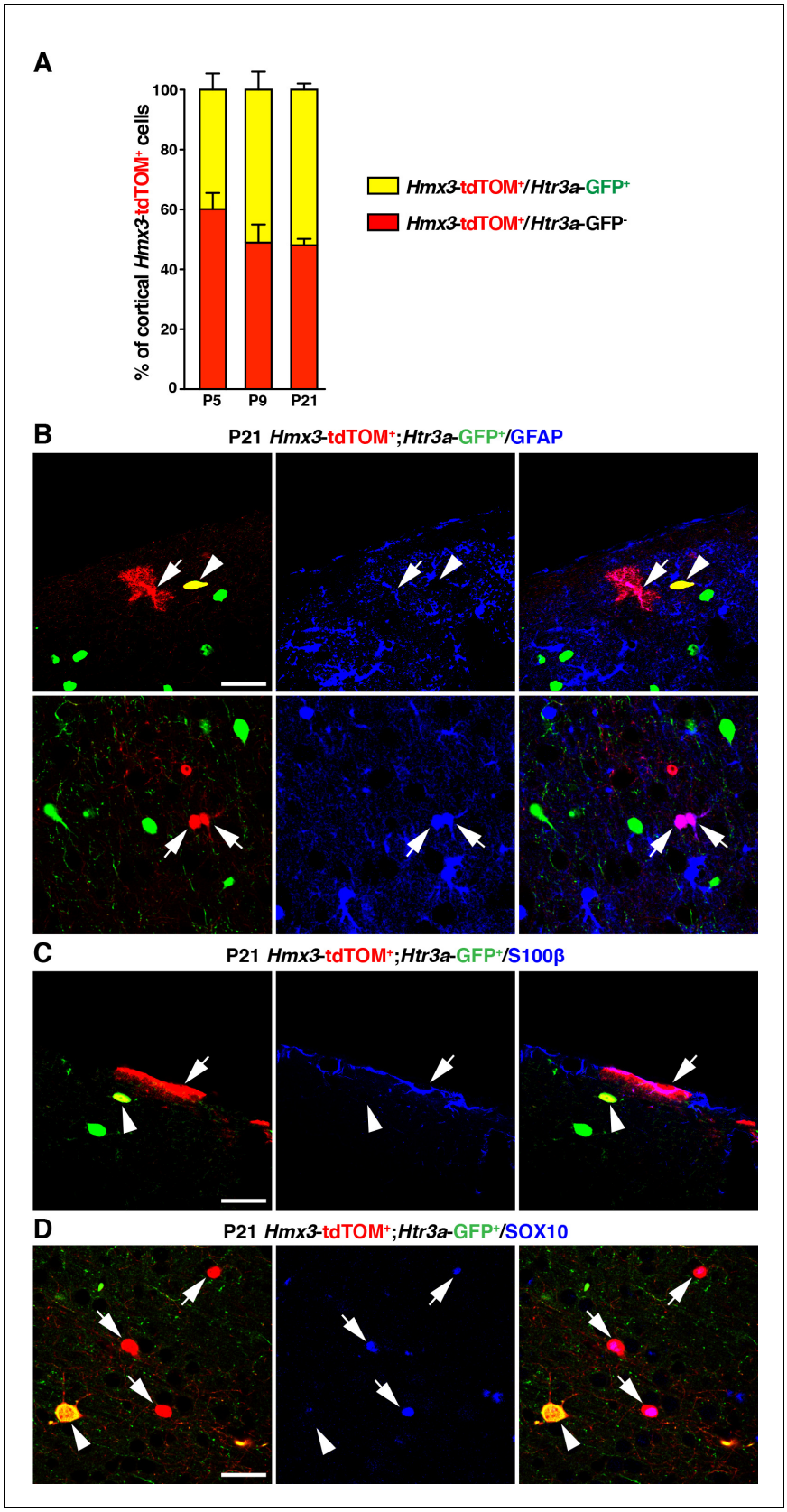

Figure 2—figure supplement 3. *Hmx3*; tdTOM+ cells negative for *Htr3a*-GFP often express glial markers. (**A**) The fraction of *Hmx3*; tdTOM+ cells negative for *Htr3a*-GFP is relatively stable across postnatal ages. (**B–D**) *Hmx3*;

Figure 2—figure supplement 3 continued on next page

Figure 2—figure supplement 3 continued

tdTOM+ cells negative for *Htr3a*-GFP express the astrocytic markers GFAP (B; arrows), S100β (C; arrow) and the oligodendrocytic transcription factor SOX10 (D; arrows). In contrast, *Hmx3*; tdTOM+/*Htr3a*-GFP+ cells are negative for these markers (B-D; arrowheads). Scale bar: 50 µm in B, C, D.

DOI: https://doi.org/10.7554/eLife.32017.008

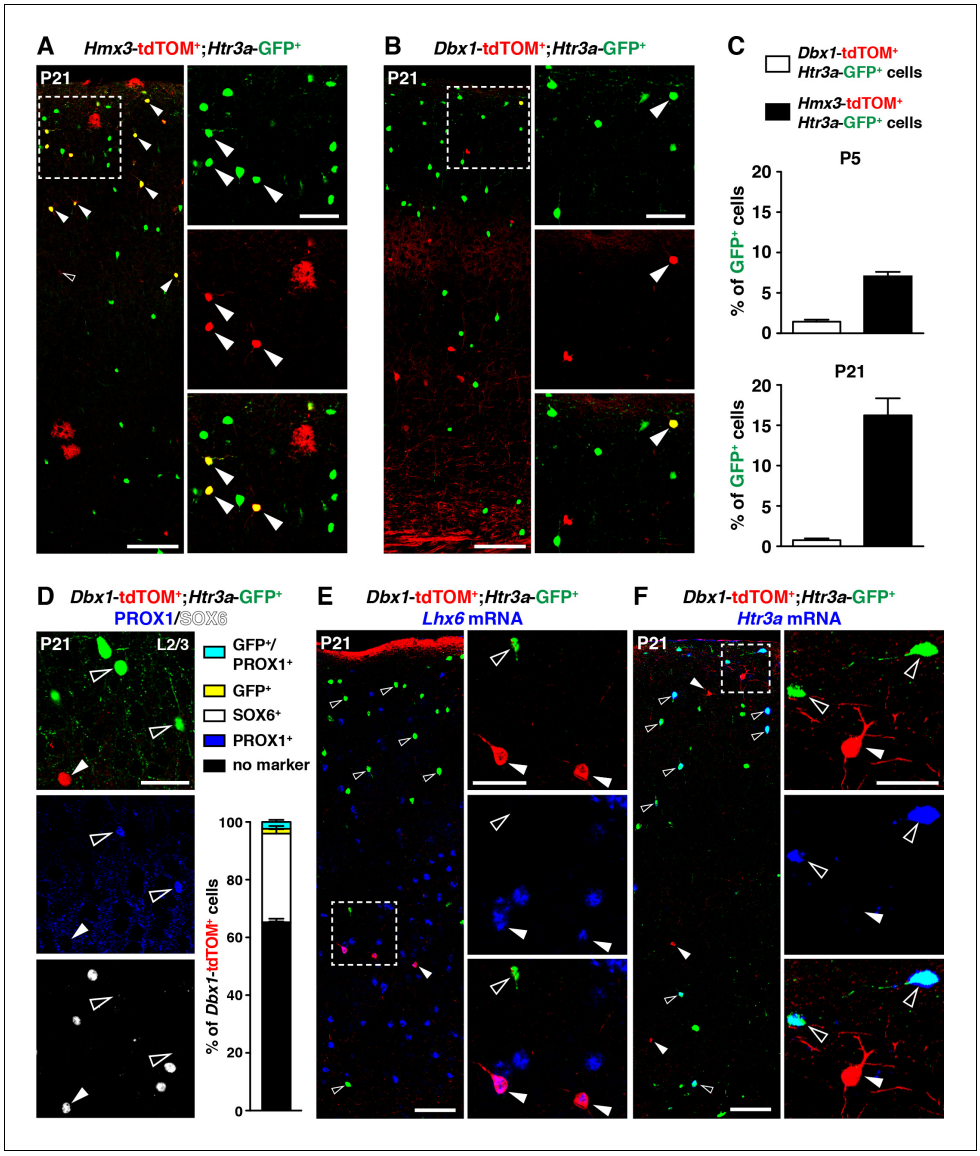

Figure 3. 5-HT_{3A}R-expressing interneurons (INs) largely originate from *Hmx3+* but not *Dbx1+* cells. (**A–C**) A consistent fraction of cortical *Htr3a*-GFP+ INs co-labels with *Hmx3*; tdTOM (A, arrowheads) at P5 and P21, whereas only a minimal fraction does with *Dbx1*; tdTOM (B, arrowhead). (**D**) *Dbx1*; tdTOM+ INs express the MGE-enriched TF SOX6 (arrowhead) but not the CGE-enriched TF PROX1 (open arrowheads). Only a minimal fraction of *Dbx1*; tdTOM+ co-labelled for *Htr3a*-GFP, among which the majority were PROX1+. (**E–F**) *In situ* hybridization showing that *Dbx1*; tdTOM+ INs express the transcript for the MGE-enriched TF *Lhx6* (E, arrowheads) whereas *Htr3a*-GFP + INs do not (E, open arrowheads). In contrast, *Dbx1*; tdTOM+ INs do not express the *Htr3a* transcript (F, arrowheads) whereas *Htr3a*-GFP+ INs do (F, open arrowheads). Scale bars: 100 μm in A, B, E, F: low magnified images; 50 μm in A, B, D, E, F: high magnified images.

DOI: https://doi.org/10.7554/eLife.32017.011

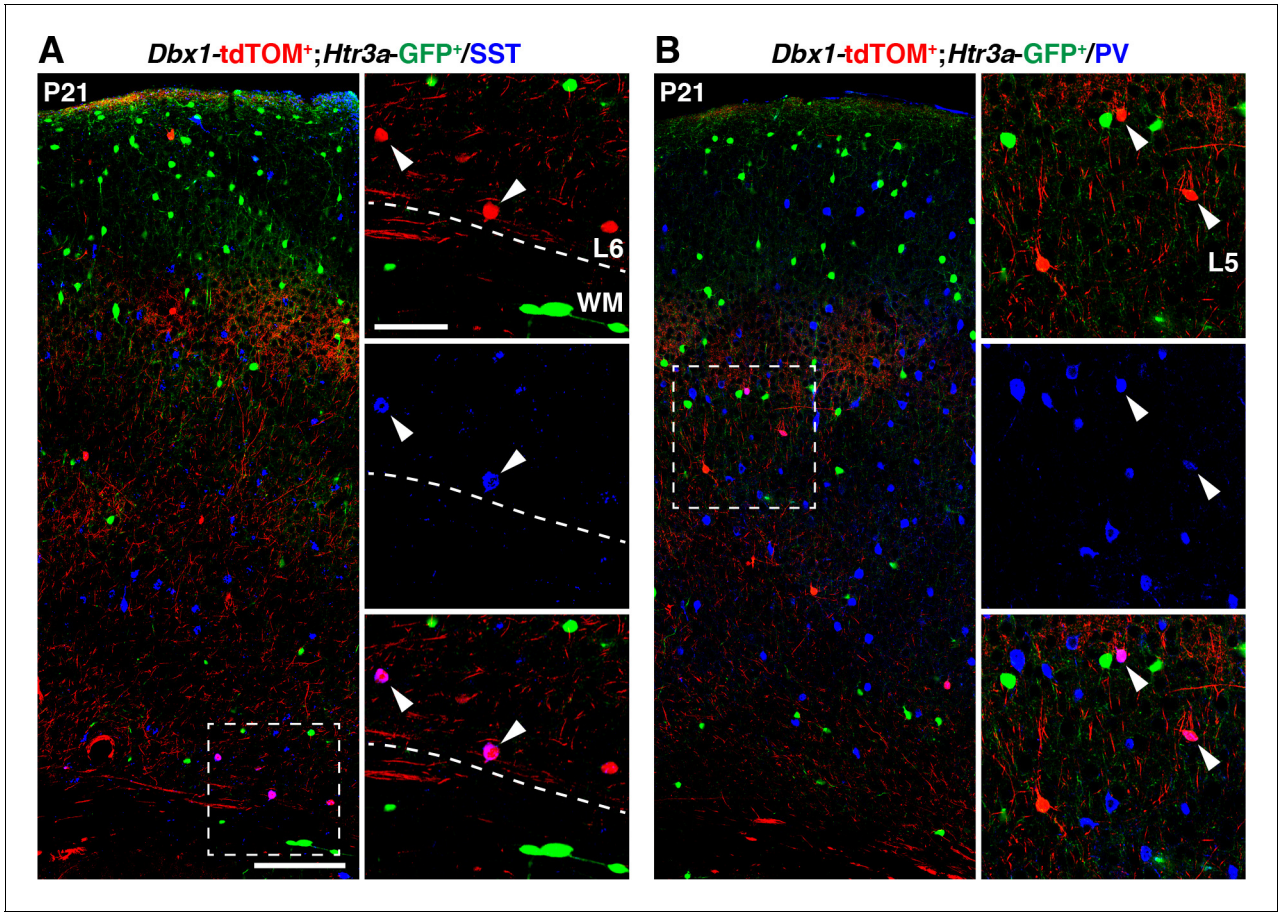

Figure 3—figure supplement 1. Interneurons (INs) derived from *Dbx.1*+ cells express MGE-enriched markers. (**A–B**) *Dbx1*; tdTOM+ cells negative for *Htr3a*-GFP express the neurochemical markers somatostatin (SST) (A, arrowheads) and parvalbumin (PV) (B, arrowheads). WM: white matter. Scale bars: 100 μm in A, B: low magnified images; 50 μm in A, B: high magnified images.

DOI: https://doi.org/10.7554/eLife.32017.012

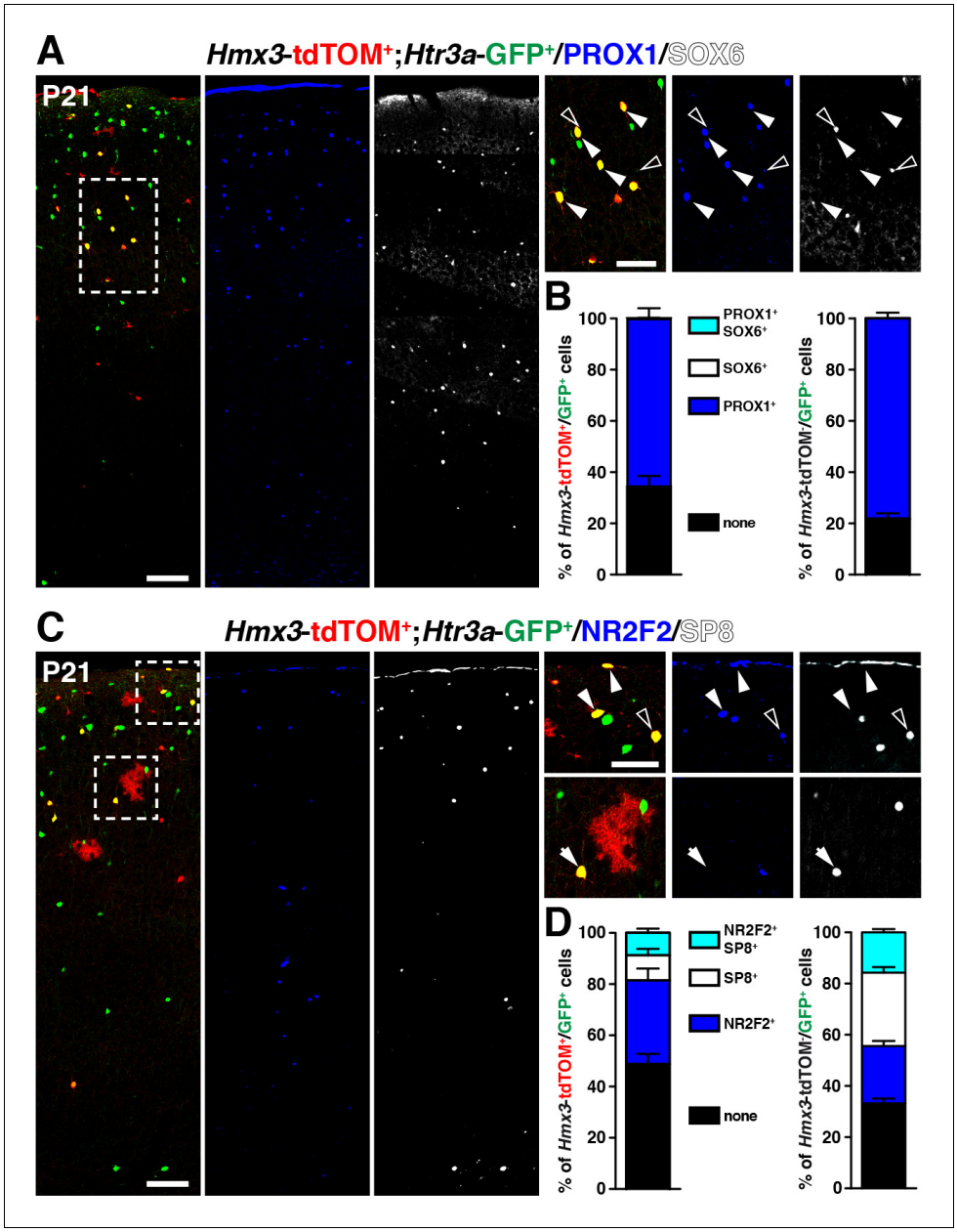

Figure 4. *Hmx3*; tdTOM+/*Htr3a*-GFP+ cortical interneurons (INs) express markers related to the CGE but not to the MGE. (**A–B**) *Hmx3*; tdTOM+/*Htr3a*-GFP+ INs express the CGE-enriched TF PROX1 (A; arrowheads) but not the MGE-related TF SOX6 (A; open arrowheads) similarly to *Htr3a*-GFP+ INs that do not derive from *Hmx3*+ cells (B, right graph). (**C–D**) *Hmx3*; tdTOM+/*Htr3a*-GFP+ cells express the CGE-enriched TFs NR2F2 (arrowheads) and (open arrowheads)/or SP8 (arrow). *Htr3a*-GFP+ derived from *Hmx3*+ cells are biased towards NR2F2 expression, in comparison to *Htr3a*-GFP+ INs that do not co-label with *Hmx3*; tdTOM (D, blue bars). Scale bars: 100 μm in A, C: low magnified images; 50 μm in A, C: high magnified images.

DOI: https://doi.org/10.7554/eLife.32017.014

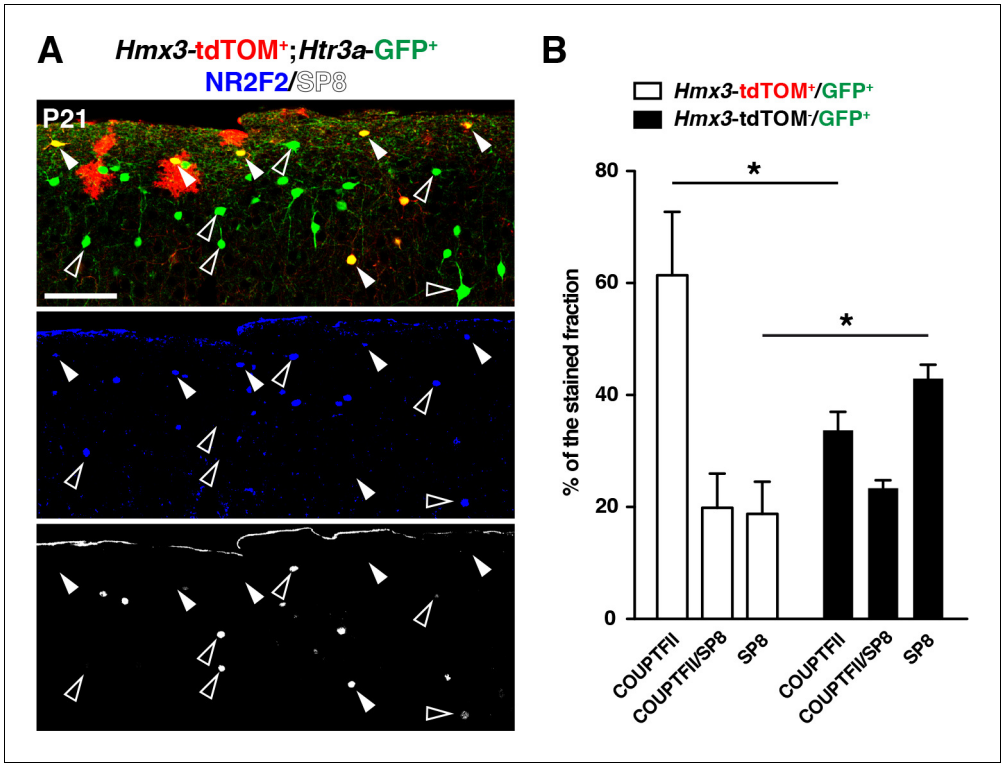

Figure 4—figure supplement 1. *Hmx3*; tdTOM+/*Htr3a*-GFP+ cortical interneurons (INs) display a combinatorial expression of NR2F2 and SP8 that is biased toward NR2F2. (**A**) *Hmx3*; tdTOM+/*Htr3a*-GFP+ INs (A; arrowheads) express significantly (one-way ANOVA; *p<0.05) more NR2F2 alone and less SP8 alone as compared to *Htr3a*-GFP + INs negative for *Hmx3*; tdTOM (A; open arrowheads). Scale bar: 100 μm in A.

DOI: https://doi.org/10.7554/eLife.32017.015

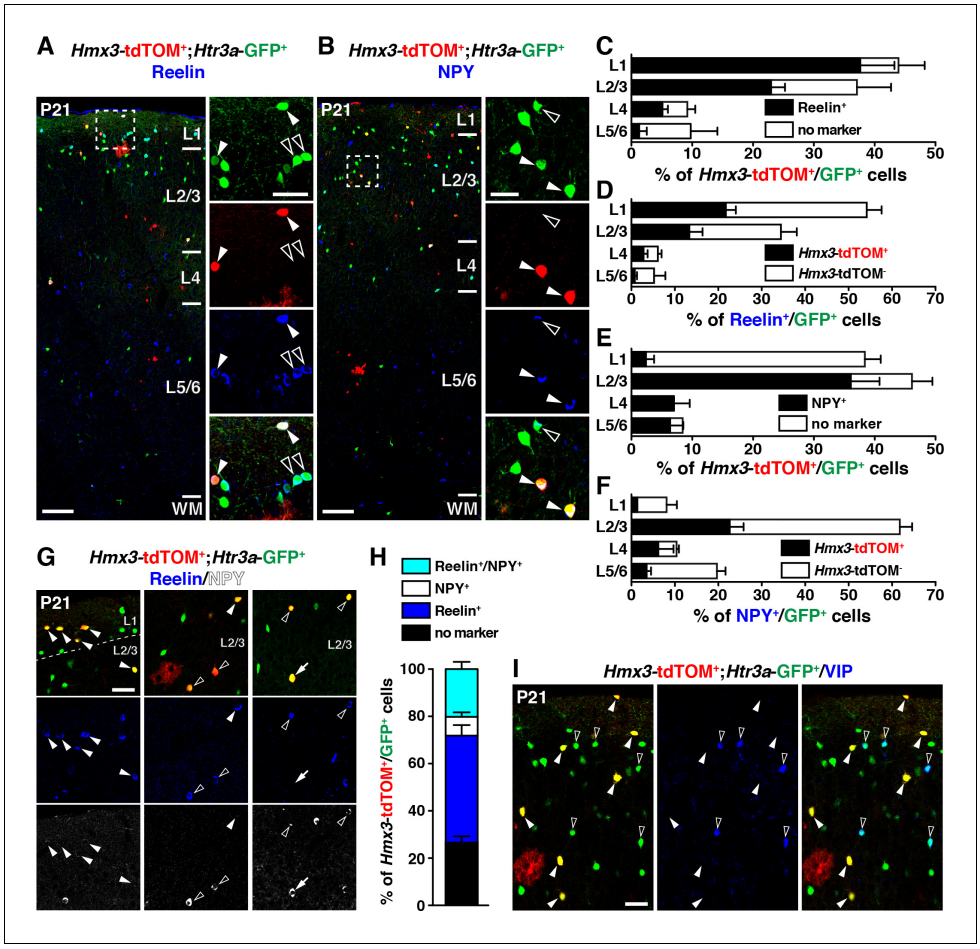

Figure 5. *Hmx3*; tdTOM+/*Htr3a*-GFP+ cortical interneurons (INs) express reelin and NPY but not VIP. (**A–F**) *Hmx3*; tdTOM+/*Htr3a*-GFP+ INs are stained with the neurochemical markers reelin (A, arrowheads) and NPY (B, arrowheads) as well as *Htr3a*-GFP+ cells negative for *Hmx3*; tdTOM (open arrowheads). Note that reelin-positive *Hmx3*; tdTOM+/*Htr3a*-GFP+ INs are preferentially found in L1-3 (**C**) whereas NPY-expressing *Hmx3*; tdTOM+/*Htr3a*-GFP+ INs are mainly found in L2-6 (**E**). *Hmx3*; tdTOM+/*Htr3a*-GFP+ INs account for more than one third of all reelin-positive *Htr3a*-GFP+ (**D**) and of all NPY-positive *Htr3a*-GFP+ cells (**F**). (**G–H**) *Hmx3*; tdTOM+/*Htr3a*-GFP + INs mainly express reelin (G, arrowheads) or reelin and NPY (G, open arrowheads) but to a smaller extend only NPY (G, arrow). (**I**) *Hmx3*; tdTOM+/*Htr3a*-GFP+ INs do not express VIP (arrowheads), whereas *Htr3a*-GFP+ INs negative for *Hmx3*; tdTOM do (open arrowheads). WM: white matter. Scale bars: 100 μm in A, B: low magnified images; 50 μm in A, B: high magnified images, G, I.

DOI: https://doi.org/10.7554/eLife.32017.017

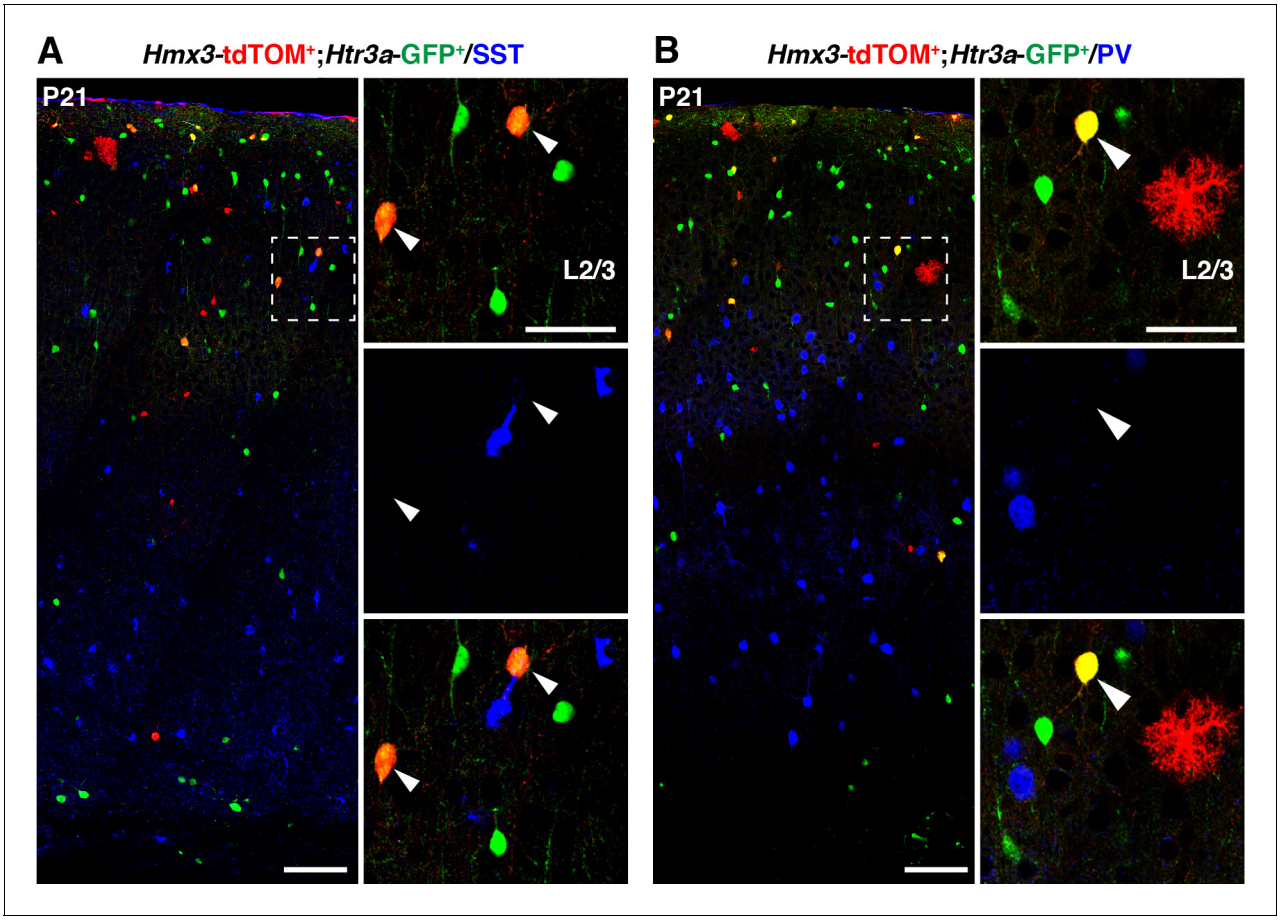

Figure 5—figure supplement 1. *Hmx3*; tdTOM+/*Htr3a*-GFP+ do not express MGE-enriched markers. (**A–B**) *Hmx3*; tdTOM+/*Htr3a*-GFP+ cells do not express the neurochemical markers somatostatin (SST) (A, arrowheads) and parvalbumin (PV) (B, arrowheads). WM: white matter. Scale bars: 100 μm in A, B: low magnified images; 50 μm in A, B: high magnified images.

DOI: https://doi.org/10.7554/eLife.32017.018

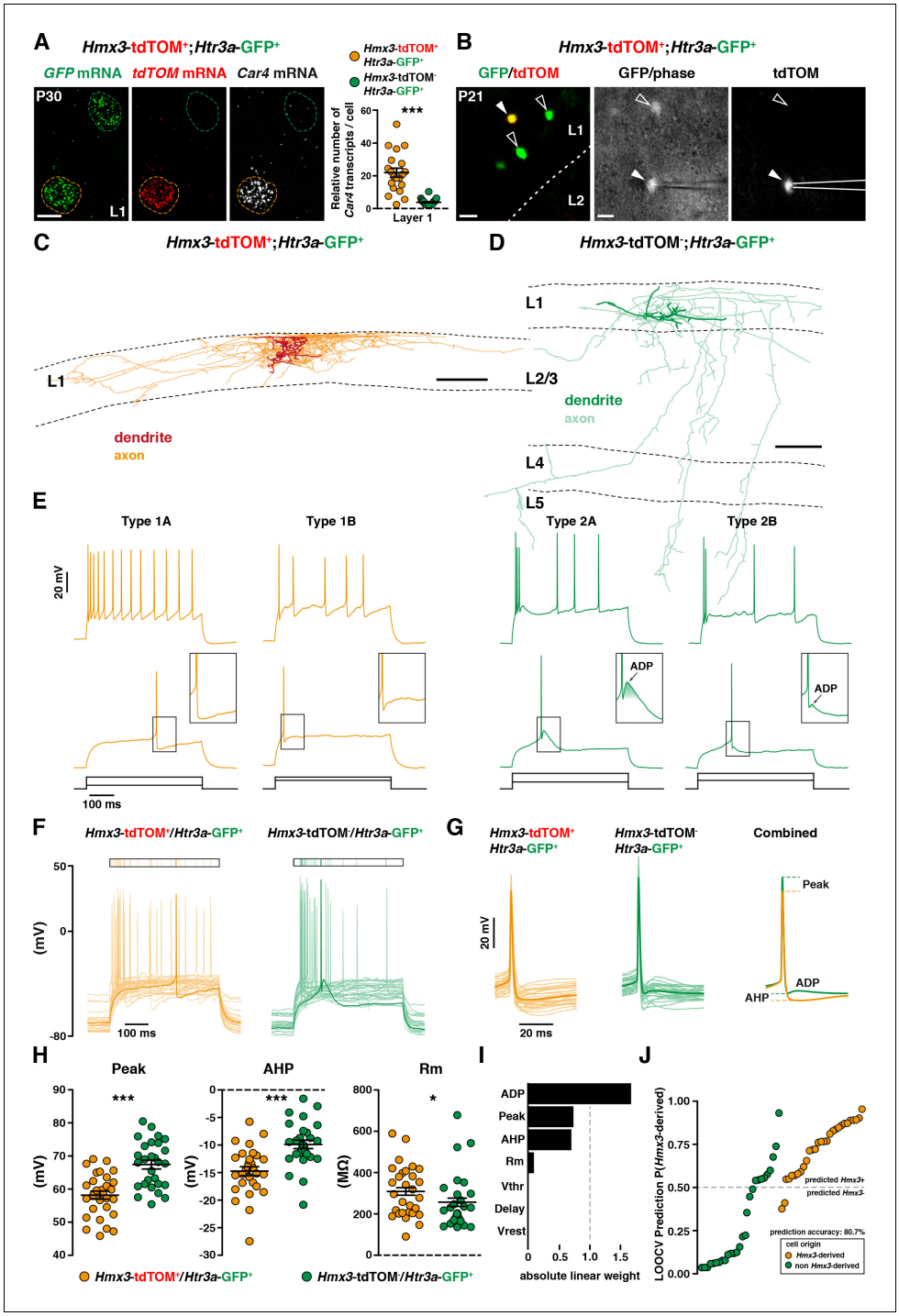

Figure 6. *Hmx3*; tdTOM+/*Htr3a*-GFP+ cortical interneurons (INs) in layer 1(L1) display the molecular, morphological and electrophysiological features of neurogliaform cells (NGCs). (**A**) RNAscope multiplex fluorescent hybridization for *tdTOM*, *GFP* and *Car4* transcripts on P30 brains showing that L1 *Hmx3*; tdTOM+/*Htr3a*-GFP+ INs express *Car4* at significantly higher levels (orange outline) as compared to *Htr3a*-GFP+ INs negative for tdTOM (green outline) (***p<0.0001; Mann-Whitney test). (**B**) Example of a L1 *Hmx3*; tdTOM+/*Htr3a*-GFP+ cell (arrowhead) or *Htr3a*-GFP+ INs negative for tdTOM (open arrowheads) checked before patching (left image). Example of a patched *Hmx3*; tdTOM+/*Htr3a*-GFP+ IN (middle and right images, arrowhead). (**C**) Illustrative reconstruction of a *Hmx3*; tdTOM+/*Htr3a*-GFP+ IN in L1 displaying the characteristic morphology of an elongated NGC with dense axonal ramifications restricted to L1. (**D**) Illustrative reconstruction of a *Htr3a*-GFP+ IN negative for tdTOM in L1 displaying the characteristic morphology of single bouquet-like cell (SBC) with axonal

Figure 6 continued on next page

Figure 6 continued

ramifications extending deep into L5. (**E**) Illustrative traces from recorded *Hmx3*; tdTOM+/*Htr3a*-GFP+ INs (orange) and *Htr3a*-GFP+ INs negative for tdTOM (green), showing the first action potentials (APs) at rheobase and trains of APs at higher current injections. (**F**) Superimposed single AP traces at rheobase of all *Hmx3*; tdTOM +/*Htr3a*-GFP+ INs (orange) and *Htr3a*-GFP+ INs negative for tdTOM (green). Thick traces correspond to type 1A and type 2A examples in E. (**G**) Same traces as in (**F**), aligned to the AP, with a lower time scale. Thin lines are individual cell traces and thick lines are trace averages. The average traces on the right are aligned to the threshold potential (Vthr). (**H**) Plots of AP peak amplitude (Peak; ***p<0.0001; unpaired t-test), after hyperpolarization potential amplitude (AHP; ***p<0.0001; unpaired t-test) and membrane resistance (Rm; *p=0.0318; Mann-Whitney test) showing significant differences between the two cell types. (**I**) Absolute linear weights assigned by the classification model trained on all cells with standardized electrophysiological properties. (**J**) Prediction probabilities estimated by the classifier on the cell left out in the leave-one-out-cross-validation (LOOCV) loop. Cells are ordered on the x-axis by origin and prediction value, and the color code reflect their origin. Cells above the probability threshold 0.5 are more likely to be *Hmx3*-derived according to the model. Scale bars: 10 µm A; 20 µm in B; 100 µm C, D.

DOI: https://doi.org/10.7554/eLife.32017.020

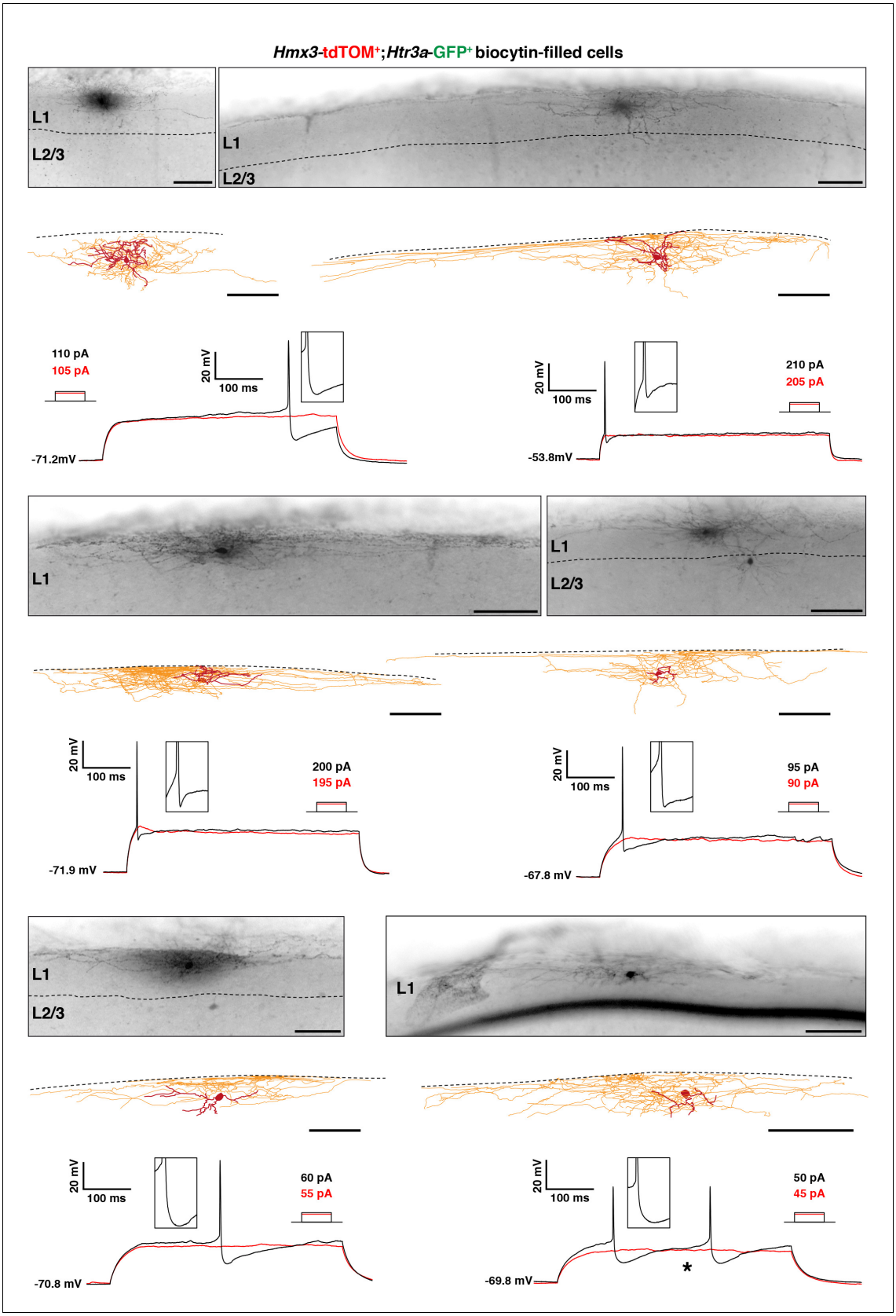

Figure 6—figure supplement 1. *Hmx3*; tdTOM+/*Htr3a*-GFP+ interneurons (INs) in layer 1 (L1) display the characteristic morphology of elongated neurogliaform cells (eNGCs). Illustrative images confirming location of the cells, morphological reconstructions and electrophysiological traces of *Hmx3*;

Figure 6—figure supplement 1 continued on next page

Figure 6—figure supplement 1 continued

tdTOM+/*Htr3a*-GFP+ INs in L1. All cells have the morphology of eNGCs with dense axonal ramifications mostly restricted to layer 1. One cell (*) was excluded from the analysis of electrophysiological properties due to the presence of two peaks at the first 5 pA increment showing an action potential, but still its biocytin filling was good enough for morphological tracing (bottom right). Scale bars: 100 μm in all brightfield images and reconstructions.
DOI: https://doi.org/10.7554/eLife.32017.021

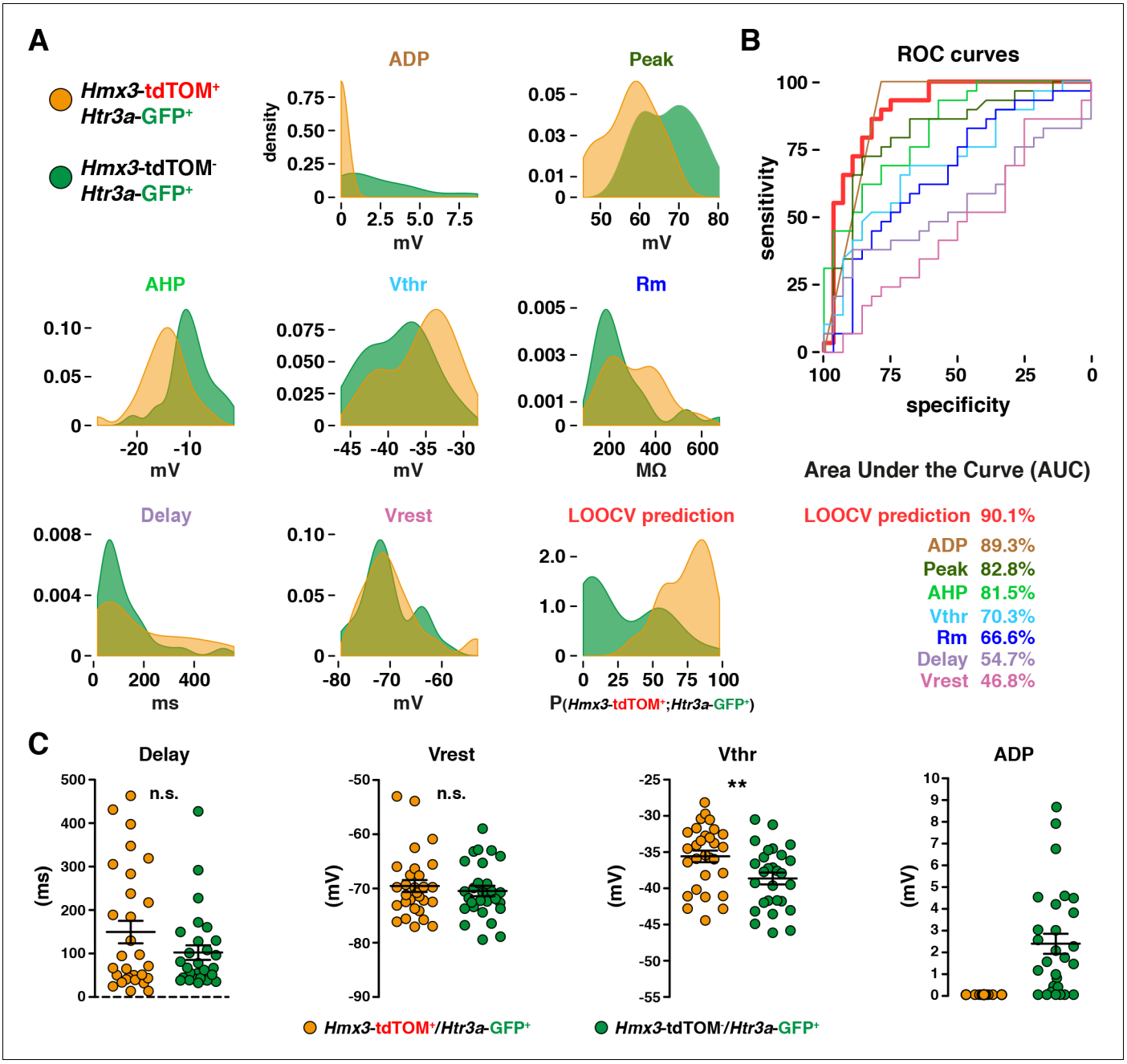

Figure 6—figure supplement 2. Prediction model parameters and electrophysiological features of *Hmx3*; tdTOM+/*Htr3a*-GFP+ interneurons (INs) in layer 1. (**A**) Density plots of the electrophysiological values as well as of the LOOCV prediction probabilities for *Hmx3*-derived cells and non *Hmx3*-derived cells. (**B**) Receiver operating characteristic (ROC) curve for each electrophysiological property and on prediction probabilities obtained by LOOCV. (**C**) Significant difference is found between *Hmx3*-derived cells and non *Hmx3*-derived cells for threshold potential (Vthr; **p=0.0097; unpaired t-test) but not for delay to the first action potential (Delay; p=0.55; Mann-Whitney test) and resting potential (Vrest; p=0.68; Mann-Whitney test). Afterdepolarization potential (ADP) is0 for all *Hmx3*-derived cells.

DOI: https://doi.org/10.7554/eLife.32017.022

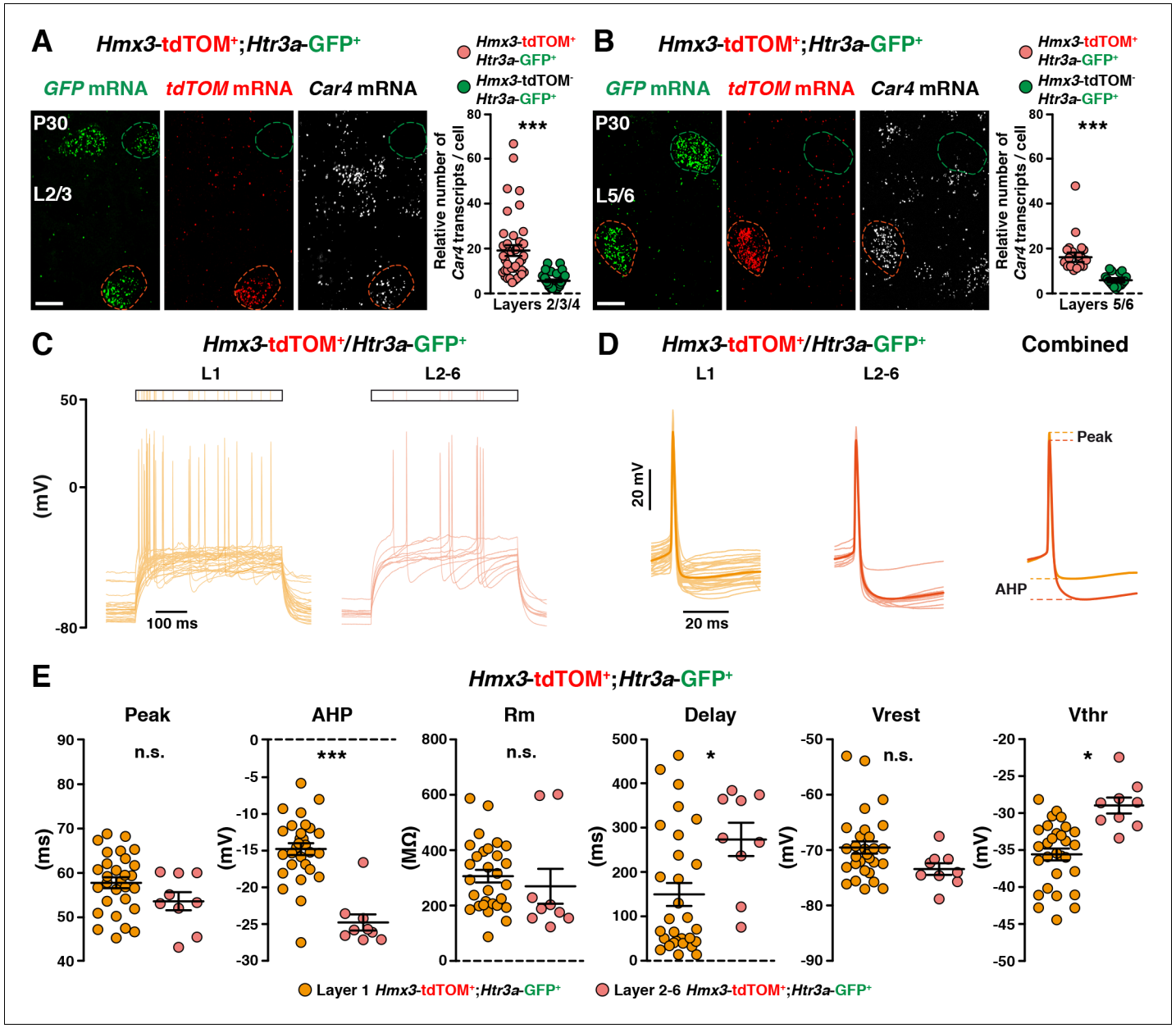

Figure 6—figure supplement 3. *Hmx3*; tdTOM+/*Htr3a*-GFP+ interneurons (INs) in cortical layers 2–6 (L2-6) display molecular and electrophysiological properties of NGCs. (**A, B**) RNAscope multiplex fluorescent hybridization for *tdTOM*, *GFP* and *Car4* transcripts on P30 brains showing that *Hmx3*; tdTOM+/*Htr3a*-GFP+ INs (red outline) express *Car4* at significantly higher levels in L2–4 (A, ***p<0.0001; Mann-Whitney test) and L5/6 (B, ***p<0.0001; Mann-Whitney test) as compared to *Htr3a*-GFP+ INs negative for tdTOM (green outline). (**C**) Superimposed single AP traces at rheobase of *Hmx3*; tdTOM+/*Htr3a*-GFP+ INs recorded in L1 (orange) and in L2–6 (red). *Hmx3*; tdTOM+/*Htr3a*-GFP+ INs from L2–6 exhibit more late-spiking profile. (**D**) Same traces as in (**C**), aligned to the AP, in a lower time scale. Thin lines are individual cell traces and thick lines are trace averages. The average traces on the right are aligned to the threshold potential (Vthr). (**E**) As compared to L1 cells, *Hmx3*; tdTOM+/*Htr3a*-GFP+ INs in L2–6 display significant differences in afterhyperpolarization amplitude (AHP; ***p=0.0001; Mann-Whitney test), delay to the first action potential (Delay; *p=0.0202; unpaired t-test) and Vthr (*p=0.0002; unpaired t-test). No significant differences were found between *Hmx3*; tdTOM+/*Htr3a*-GFP+ INs in L2–6 and L1 for peak amplitude (Peak; p<0.1058; unpaired t-test), membrane resistance (Rm; p=0.5011; unpaired t-test) and resting potential (Vrest; p=0.7056; unpaired t-test), Scale bars: 10 μm in all.

DOI: https://doi.org/10.7554/eLife.32017.023

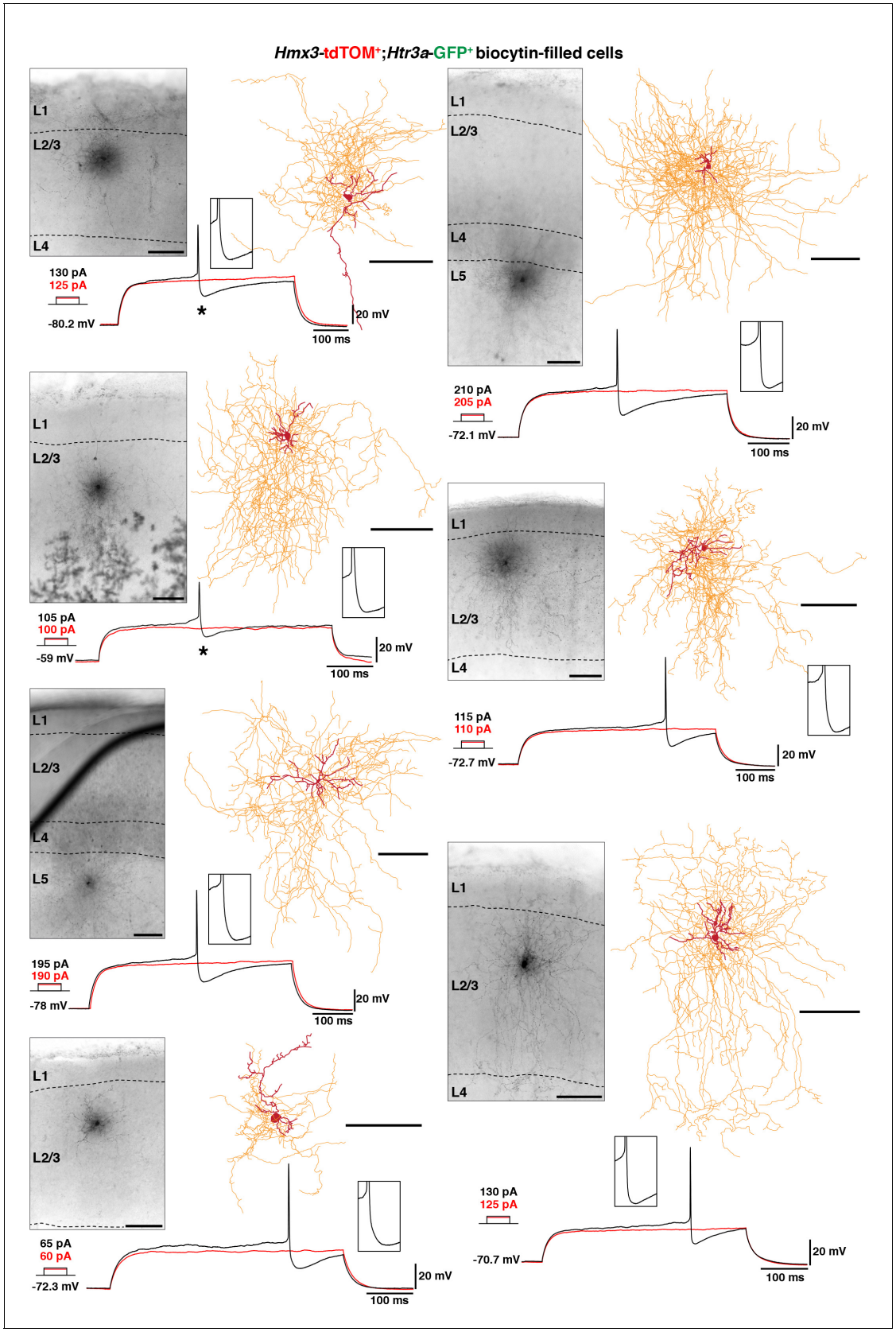

Figure 6—figure supplement 4. *Hmx3*; tdTOM+/*Htr3a*-GFP+ interneurons (INs) in cortical layers 2–6 (L2-6) display the characteristic morphology of NGCs. Illustrative images confirming location of the cells, morphological reconstructions and electrophysiological traces of *Hmx3*; tdTOM+/*Htr3a*-GFP

Figure 6—figure supplement 4 continued on next page

Figure 6—figure supplement 4 continued

+ INs in L2–6. All cells have the morphology of NGCs with dense axonal ramifications extending throughout layers. Two cells (*) were excluded from the analysis of electrophysiological properties due to high series resistance, but still their biocytin filling was good enough for morphological tracing (left, upper two panels). Scale bars: 100 μm in all.

DOI: https://doi.org/10.7554/eLife.32017.024

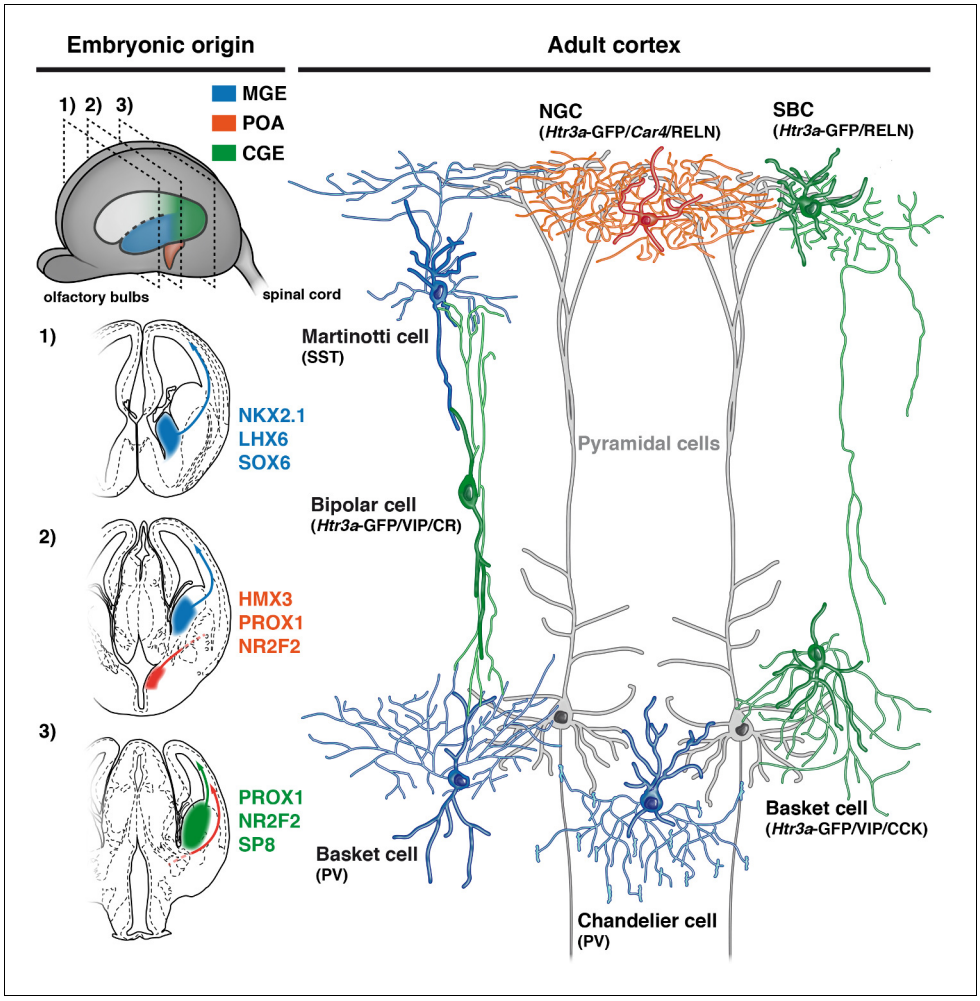

Figure 7. Developmental origin of cardinal classes of cortical interneurons. The Martinotti somatostatin (SST) cell, the parvalbumin (PV) basket cell and the PV+ chandelier cell originate from NKX2.1+ progenitors of the medial ganglionic eminence (MGE, blue) and rely on the transcription factors (TFs) LHX6 and SOX6. The *Htr3a*-GFP/reelin (RELN) single-bouquet cell (SBC), the *Htr3a*-GFP/vasointestinal peptide (VIP)/cholecystokinin (CCK) basket cell and the *Htr3a*-GFP/VIP/calretinin (CR) bipolar cell are derived from cells located in the caudal ganglionic eminence (CGE, green) that express the TFs PROX1, NR2F2 and SP8. The RELN/*Car4*/*Htr3a*-GFP neurogliaform cell (NGC) is specifically derived from *Hmx3*+ cells located in the preoptic area (POA, orange) and express the TFs PROX1 and NR2F2.

DOI: https://doi.org/10.7554/eLife.32017.029